Desynchronization in diluted neural networks

Rüdiger Zillmer,[1,*] Roberto Livi,[2,3,†] Antonio Politi,[4,5,‡] and Alessandro Torcini[4,5,§]
[1]*INFN Sezione Firenze, via Sansone 1, I-50019 Sesto Fiorentino, Italy*
[2]*Dipartimento di Fisica, Universitá di Firenze, via Sansone 1, I-50019 Sesto Fiorentino, Italy*
[3]*Sezione INFN, Unita' INFM e Centro Interdipartimentale per lo Studio delle Dinamiche Complesse, via Sansone 1, I-50019 Sesto Fiorentino, Italy*
[4]*Istituto dei Sistemi Complessi, CNR, CNR, via Madonna del Piano 10, I-50019 Sesto Fiorentino, Italy*
[5]*Centro Interdipartimentale per lo Studio delle Dinamiche Complesse, via Sansone 1, I-50019 Sesto Fiorentino, Italy*
(Received 7 March 2006; published 5 September 2006)

The dynamical behavior of a weakly diluted fully inhibitory network of pulse-coupled spiking neurons is investigated. Upon increasing the coupling strength, a transition from regular to stochasticlike regime is observed. In the weak-coupling phase, a periodic dynamics is rapidly approached, with all neurons firing with the same rate and mutually phase locked. The strong-coupling phase is characterized by an irregular pattern, even though the maximum Lyapunov exponent is negative. The paradox is solved by drawing an analogy with the phenomenon of "stable chaos," i.e., by observing that the stochasticlike behavior is "limited" to an exponentially long (with the system size) transient. Remarkably, the transient dynamics turns out to be stationary.

DOI: 10.1103/PhysRevE.74.036203 PACS number(s): 05.45.Xt, 84.35.+i, 87.19.La

I. INTRODUCTION

During the last few years it has become increasingly clear that understanding the behavior of many different systems passes through the comprehension of the dynamics of complex networks [1]. This is, for instance, the case of metabolic systems genetic networks, the immune response system, and neurobiological structures [1]. A particular challenge is represented by the need to unravel the mutual connections between network structure and dynamical properties. Very little is in fact known about the expected classes of behavior and their stability properties, even in systems of globally coupled identical oscillators. For this reason, and under the assumption of a structural stability of the possible scenarios, it is therefore instructive to investigate simple models, such as diluted neural networks of pulse-coupled neurons. Since it seems that inhibition plays a major role in determining the dynamics of single neocortical pyramidal neuron [2], as well as of cortical networks [3], we have chosen to examine a network of inhibitory coupled leaky integrate-and-fire neurons. More precisely, we consider the model proposed in Ref. [4], where Jin, under fairly general conditions, investigated analytically the convergence towards a periodic pattern. In this paper we study the diluted version of this model, showing that even though the dynamics is characterized by a negative maximum Lyapunov exponent [5], irregular and exponentially long transients are typically observed for a sufficiently strong coupling strength. This phenomenon is somehow analogous to what was observed in diluted networks of pulse-coupled oscillators with delay [6], although the transients therein reported are chaotic in the typical sense of the word. More precisely, we find that for small coupling amplitudes the dynamics converges, after a short transient, towards a synchronized state with all neurons firing with the same rate, but with their phases approximately uniformly distributed. This can be understood by first referring to a homogeneous network of globally coupled neurons. In that context, the mean field is found to induce an effective repulsive interaction between the neurons; as a result the asymptotic regime is characterized by an evenly spaced sequence of spikes which is known in the literature as a *splay state* [7]. As a result of random dilution, one can imagine that inhomogeneities in the mutual interactions arise which in turn lead to small nonuniformities in the interspike intervals.

On the other hand, for sufficiently large coupling amplitudes, stochasticlike transients are observed, whose duration is exponentially long with the network size. Since various indicators show that this regime is stationary, it is logical to conclude that in infinitely large networks it represents a perfectly legitimate thermodynamic phase. This is analogous to the active phase in directed percolation, whose lifetime is finite in finite systems. Even more stringent is the analogy with "stable chaos," a kind of irregular behavior discovered in coupled map lattices [8] and characterized by negative Lyapunov exponents. Since it is believed that such a pseudochaotic behavior is sustained by discontinuities of the mapping rule [9], it is natural to expect this to be true also in the present case. Quite consistently, we observe that in the presence of disorder, where neurons are no longer equivalent to one another, changes in the firing order are accompanied by discontinuities in the evolution rule.

Altogether, the transition manifests itself as a collective desynchronization phenomenon. Unfortunately, a "microscopic" linear-stability analysis does not allow identifying the threshold, since all trajectories are asymptotically stable in both regimes. Moreover, direct numerical simulations are not very effective either due to the difficulty of simulating large networks, so that the study of the critical behavior is an even more difficult task. However, the evidence of two distinct phases is rather convincing and, furthermore, the introduction of a suitable space-time representation suggests a

*Electronic address: zillmer@fi.infn.it
†Electronic address: livi@fi.infn.it
‡Electronic address: antonio.politi@isc.cnr.it
§Electronic address: alessandro.torcini@isc.cnr.it

true analogy with directed percolation that will be worth exploring in more detail.

In Sec. II, we introduce the model and the variables, while the homogeneous case of fully coupled networks is analytically investigated in Sec. III, where we also introduce a one-dimensional (1D) description of the dynamics that applies exactly in the thermodynamic limit. In Sec. IV the transient dynamics of weakly diluted networks is discussed, both by determining the transient length and analyzing its stationarity properties. The resulting two-phase scenario is then summarized in Sec. V, where we also present an effective stochastic description. Further comments about open questions and indications for future studies are finally presented in the Conclusions (Sec. VI).

II. THE MODEL

In this paper we investigate a system of N leaky integrate-and-fire (LIF) neurons, analogous to the model discussed in Ref. [4]. The state of the ith neuron is fully determined by the membrane potential $V_i(\tilde{t})$ and obeys the differential equation

$$\tau \dot{V}_i = C - V_i - \tau(V_i + W)\sum_{j=1}^{N}\sum_{m} g_{ij}\delta(\tilde{t} - \tilde{t}_j^{(m)}), \qquad (1)$$

where τ is the membrane time constant, C is the suprathreshold input current (referred to a unitary membrane resistance), and W is the reversal potential. Whenever the potential $V_j(\tilde{t})$ reaches the threshold value Θ, it is reset to $R<\Theta$, and a spike is sent to and instantaneously received by all connected neurons at time $\tilde{t}_j^{(m)}$ (the superscript m enumerates the firing events of the jth neuron). The net result of a received spike is that the membrane potential of the ith receiving neuron is decreased according to the transformation

$$V_i' + W = (V_i + W)\exp(-g_{ij}). \qquad (2)$$

As a consequence of the inhibitory connections, the potential V_i' can go below the reset value R, but Eq. (2) shows that $-W$ is a true lower bound. However, for small coupling values and in the absence of clustering phenomena (as in the present paper), it turns out that V_i is essentially bounded between R and Θ. The last ingredient defining the system dynamics is the connectivity matrix g_{ij}. Following the recent literature on randomly connected directed networks [6,10], the coupling strength is scaled to the connectivity of the receiving neuron,

$$g_{ij} = \begin{cases} G/\ell_i, & \text{if } i \text{ and } j \text{ are coupled} \\ 0, & \text{otherwise} \end{cases}; \qquad (3)$$

where G is the coupling constant and ℓ_i is the number of incoming links to neuron i. In other words, we consider the simplest type of disorder, determined just by the presence (absence) of links between neurons (notice that self-interactions are excluded, i.e., $g_{ii}=0$). As we are interested in studying networks with a given fraction r_m of missing links, there are in principle different ways of doing that: (i) each link is cut with a probability r_m; (ii) the total number N_m of cut links is fixed deterministically $[N_m=r_m N(N-1)]$; (iii) the number of cut links per neuron is fixed deterministically. Since preliminary simulations performed according to the three philosophies have given qualitatively similar results, we eventually decided to restrict our quantitative analyses to the second approach. Moreover, since we aim at understanding the possibly qualitative changes induced by disorder in the neural network dynamics, we limit ourselves to analyzing the case of weak disorder. This is done by choosing small values for the fraction r_m (typically $r_m=0.05$).

Most of the parameter values are set according to the current literature (see, e.g., [4,11]), namely: $\tau=20$ ms, $C=-45$ mV, $W=63$ mV, $\Theta=-52$ mV, and $R=-59$ mV. As a matter of fact, the only free parameters of the model are the fraction r_m and the coupling constant G, which tunes the strength of the inhibitory coupling.

The dynamical equation (1) can be recasted into a simpler form by introducing the following dimensionless parameters:

$$t = \tilde{t}/\tau, \quad v_i = (V_i - R)/(\Theta - R),$$

$$c = (C - R)/(\Theta - R), \quad w = (W + R)/(\Theta - R).$$

This amounts to rescaling Θ and R to the values 1 and 0, respectively. Moreover, for the above choice of parameter values, $c=2$ and $w=4/7$.

As a result, Eq. (1) reads

$$\dot{v}_i = c - v_i - (v_i + w)\sum_{j=1}^{N}\sum_{m} g_{ij}\delta(t - t_j^{(m)}). \qquad (4)$$

Since $w>0$, the coupling is fully inhibitory, i.e., an incoming spike lowers the potential of the receiving neuron and hence the coupling inhibits firing.

At variance with the original model in Ref. [4], where both the threshold currents C_i and the coupling constants g_{ij} are assumed to be randomly distributed, here the only source of disorder is the presence (absence) of inhibitory connections. This choice is dictated by our interest in relatively simple structures to better understand the possible scenarios. However, the most important difference concerns the coupling constant: no dependence on the system size is postulated in Ref. [4], while an inverse proportionality to the number of incoming connections is assumed here.

This latter normalization is more suited to investigate the large N limit, since it guarantees that the coupling strength remains comparable to the amplitude of the force field $(c\text{-}v)$.

By following the approach of Ref. [4], we map the original model onto a discrete-time map. Let $v_i(n)$ denote the membrane potential of the ith neuron immediately after the nth spike. Until the next spike is emitted, the network evolution corresponds to an exponential relaxation of each v_i towards c. One can easily infer from (4) that the time interval Δt_i needed by the ith neuron to reach the firing threshold $v_i=1$ is

$$\Delta t_i(n) := \ln \Gamma_i(n), \text{ with } \Gamma_i(n) = \frac{c - v_i(n)}{c - 1}. \qquad (5)$$

Let $k(n)$ denote the label of the neuron characterized by the shortest time, i.e.,

$$\Gamma_{k(n)} = \min_i \{\Gamma_i\}. \tag{6}$$

By now including the effect of the next spike, the network dynamics can be transformed into a discrete map for the quantities $\Gamma_i(n)$. In the large N (and, accordingly, ℓ_i) limit, one obtains

$$\Gamma_k(n+1) = \frac{c}{c-1}, \tag{7a}$$

$$\Gamma_i(n+1) = g_{ik}a + (1-g_{ik})\frac{\Gamma_i(n)}{\Gamma_k(n)} \quad \text{for } i \neq k, \tag{7b}$$

where

$$a := \frac{c+w}{c-1}. \tag{8}$$

The process can be iterated by finding the minimum among the $\Gamma_i(n+1)$ and so on. Therefore, $\Delta t_{k(n)}(n)$ represents the time interval between the nth and the $(n+1)$-st spike; following the standard notation, it will be denoted with $t_{\mathrm{ISI}}(n)$. On the other hand $T(m)$ denotes the time elapsed between the $(m+1)$-st spike and the previous spike emitted by the *same* neuron.

III. THE HOMOGENEOUS CASE

In this section we discuss the dynamics of homogeneous networks, i.e., $g_{ij}=G/\ell_i$ (for $i \neq j$) and $\ell_i=N$. In the absence of any disorder (globally coupled identical neurons), any initial ordering of the neuron spikes will persist at all times, because it cannot be changed by the dynamical rule.

Accordingly, after a short transient, the trajectory converges towards a periodic orbit characterized by equispaced spikes, $t_{\mathrm{ISI}}(n)=T/N$ and $T(m)=T$ for all n, m. By formally interpreting the separation between the spike time $t_j^{(m)}$ of the jth neuron and the preceding spike time $t_i^{(n)}$ of some reference neuron as a phase variable, one can summarize the scenario by stating that the single-neuron phases repel each other until an equilibrium state, characterized by a maximal and uniform separation, is attained. In the literature, this alignment is called splay state and it has been found in various models of globally coupled oscillators [7]. Such a state can be viewed as the opposite situation of a fully synchronized state, where all oscillators share the same phase. It is curious that this regime is attained in the presence of inhibitory coupling, since this property is usually associated with the propensity to synchronize instead. In fact, splay states have been found in globally coupled LIF neurons in the presence of excitatory coupling with spikes of finite width [12,13].

A. Stationary solution

Since the ordering of the neuron potentials, v_i, does not change in time, one is free to label the spiking neuron in such a way that $k(n+1)=k(n)+1 \bmod N$. It is also convenient to choose a "moving" frame, namely $j=i-n$, since the label of the spiking neuron remains constant and can thereby be set equal to 1, without loss of generality. The resulting map reads

$$\Gamma_{j-1}(n+1) = \frac{aG}{N} + \left(1 - \frac{G}{N}\right)\frac{\Gamma_j(n)}{\Gamma_1(n)}, \tag{9}$$

with the boundary condition $\Gamma_N=\tilde{c}:=c/(c-1)$. This equation admits a stationary solution, which corresponds to a regime of evenly spaced spikes, i.e., a splay state [7].

The fixed point of (9) is obtained by solving the recursive relation

$$\tilde{\Gamma}_{j-1} = \frac{aG}{N} + \left(1 - \frac{T+G}{N}\right)\tilde{\Gamma}_j,$$

where $\tilde{\Gamma}_1$ is approximated with $1+T/N$. In fact, from the very definition, one has $\ln \tilde{\Gamma}_1 = t_{\mathrm{ISI}} = T/N$, so that T is the (constant) single neuron interspike interval. By iterating the above equation backward from the initial condition $\tilde{\Gamma}_N=\tilde{c}$, one obtains

$$\tilde{\Gamma}_{N-n} = \frac{aG}{T+G}\left[1 - e^{-(T+G)n/N}\right] + \tilde{c}e^{-(T+G)n/N}. \tag{10}$$

The value of T can be finally determined by imposing the condition

$$\tilde{\Gamma}_1 = 1 + T/N. \tag{11}$$

By neglecting first-order corrections in $1/N$, one obtains

$$1 = \frac{aG}{T+G}\left[1 - e^{-(T+G)}\right] + \tilde{c}e^{-(T+G)}. \tag{12}$$

B. Linear stability

Let us consider the evolution of an infinitesimal perturbation $\gamma_j(n)$ of the fixed point $\tilde{\Gamma}_j$. From the linearization of Eq. (9) it follows that $\gamma_j(n)$ satisfies the recursive relation

$$\gamma_{j-1}(n+1) = \left(1 - \frac{T+G}{N}\right)\left[\gamma_j(n) - \left(1 - \frac{T}{N}\right)\tilde{\Gamma}_j\gamma_1(n)\right], \tag{13}$$

where higher order corrections in $1/N$ are neglected. Because of the reset $\tilde{\Gamma}_N=c/(c-1)$, it is natural to impose the boundary condition $\gamma_N=0$. By further setting $\gamma_j(n+1)=\mu\gamma_j(n)$, one obtains the eigenvalue equation,

$$\gamma_j - \left(1 - \frac{T}{N}\right)\tilde{\Gamma}_j\gamma_1 - \tilde{\mu}\gamma_{j-1} = 0, \tag{14}$$

where

$$\tilde{\mu} := \frac{\mu}{1-(T+G)/N}.$$

By iterating the above equation and imposing the boundary condition, we find that $\tilde{\mu}$ satisfies the equation

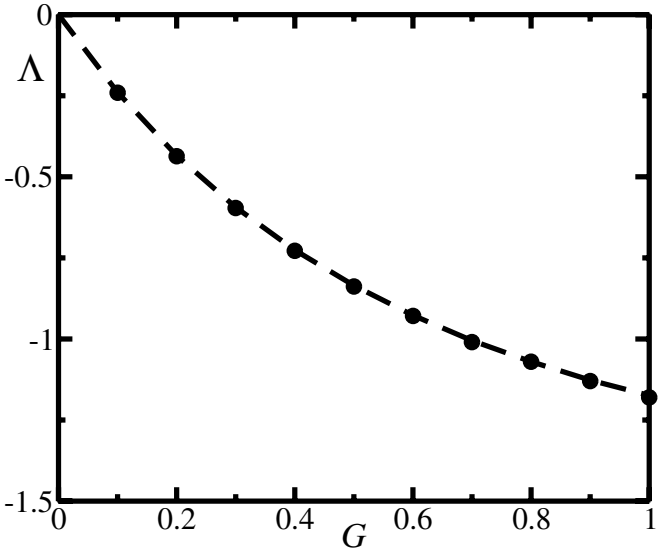

FIG. 1. The maximal Lyapunov exponent Λ corresponding to (9) for $r_p=0$, $c=2$, $w=4/7$ vs the coupling G. The dashed line refers to the analytical expression (17) and the symbols to numerical estimates.

$$\tilde{\mu}^{N-1} + \left(1 - \frac{T}{N}\right) \sum_{j=0}^{N-2} \tilde{\Gamma}_{N-j} \tilde{\mu}^j = 0.$$

By inserting the expression of $\tilde{\Gamma}_{N-j}$ [see Eq. (10)] and using the condition (12), we find that for $N \gg 1$

$$\tilde{\mu} = -1 - \frac{\ln \tilde{c}}{N}; \tag{15}$$

which yields the expression of the Lyapunov exponent of the discrete map,

$$\lambda = \ln |\mu| = -\frac{1}{N}[T + G - \ln \tilde{c}]. \tag{16}$$

The Lyapunov exponent of the original system is finally obtained by rescaling time with the interspike interval T/N,

$$\Lambda = \frac{N}{T} \ln |\mu| = -1 - \frac{G - \ln \tilde{c}}{T}. \tag{17}$$

In Fig. 1 we plot Λ and compare it with numerical results for different values of the coupling G. It is worth recalling that $T \equiv T(G)$ as from Eq. (12).

C. Continuous approach

In the large N limit, the discrete time (n) and space (j) variables can be transformed into continuous ones by introducing

$$x = j/N, \quad x \in [0,1], \quad \tau = n/N.$$

As a result, by neglecting $1/N^2$ terms, Eq. (9) can be written as

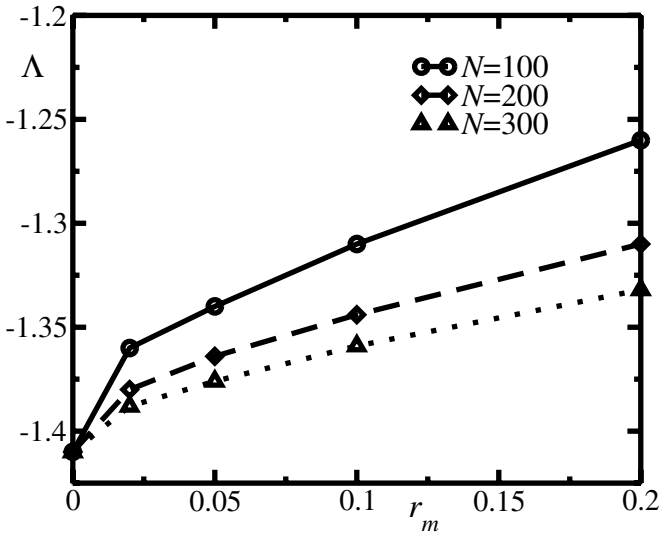

FIG. 2. The maximal Lyapunov exponent Λ for different values of the cut ratio r_m and for three values of the system size. The data refer to a coupling $G=2$.

$$-\frac{\partial \Gamma}{\partial x} + \frac{\partial \Gamma}{\partial \tau} = -(T+G)\Gamma + aG, \tag{18}$$

where we have made use of Eq. (11). The boundary conditions now read $\Gamma(0,\tau)=1$ and $\Gamma(1,\tau)=\tilde{c}$. The stationary solution corresponds to the fixed point of (9) and reads

$$\tilde{\Gamma}(x) = \left(1 - \frac{aG}{T+G}\right) e^{(T+G)x} + \frac{aG}{T+G}. \tag{19}$$

The period T is defined by imposing the boundary condition at $x=1$, i.e.,

$$\left(1 - \frac{aG}{T+G}\right) e^{(T+G)} + \frac{aG}{T+G} = \tilde{c}.$$

This result is consistent with Eq. (12). Thus, we see that the evolution equation of the globally coupled homogeneous network can be reduced to a $1+1$ dimensional partial differential equation. We shall see later that this analogy proves fruitful to interpret the phase transition discussed in the following sections.

IV. TRANSIENT DYNAMICS

From now on we study the dynamics of model (4) when a small fraction r_m of links is removed. It turns out that in this case a much more interesting and complex dynamics may emerge when the coupling strength is increased, even though the Lyapunov exponent remains negative. However, at variance with the proceeding section, here we can rely on numerical simulations only.

We expect that the weak amount of disorder induced by the random pruning of directed links reduces the coupling strength among the neurons and correspondingly increases the value of Λ with respect to the fully coupled case. The results plotted in Fig. 2 show that this is indeed the case, as

the Lyapunov exponent is found to increase with the pruning ratio r_m. Nevertheless, Λ remains negative up to $r_m=0.2$. Moreover, numerical simulations indicate that Λ remains finite in the thermodynamic limit $N\to\infty$.

As a result, sooner or later the dynamics must converge towards a stable periodic orbit. In Ref. [4], Jin has derived an upper bound for the transient length in the case of generic disorder. More precisely, he finds that the number of spikes preceding a periodic pattern is

$$P \approx N^q + (q-1), \tag{20}$$

where, in the large N limit, and with reference to our notations,

$$q = -\ln(\Delta/8a^3)/g_{min} + 1,$$

$$g_{min} = \min_{i,j}\{g_{i,j}\}, \text{ and finally,}$$

$$\Delta = \min_{n=1,\ldots,\infty} \min_{j\neq k(n)} [\Gamma_j(n) - \Gamma_{k(n)}(n)].$$

Although the N dependence expressed by Eq. (20) superficially looks like a power law, it is in fact much faster. First of all, if the coupling strength scales as $1/N$ (as it is assumed here), the exponent q grows linearly with N. Incidentally, this is true also in the fully coupled regime, where we have seen that the transient is, in reality, much shorter. A second reason is that in systems with some pruning (like here), g_{min} is equal to 0 and the exponent q would be actually equal to infinity. Finally, Δ, which is the minimal distance between the membrane potential of the two neurons that are closest to the firing threshold, cannot be larger than $1/N$. This leads to an additional logarithmic growth of the exponent q with N. Accordingly, we conclude that the analytic estimate contained in Ref. [4] applied to our setup is much too large an overestimation of the transient length to help us to understand when and whether a phase transition can occur.

The transient duration $t_{\rm tr}$ is determined as the smallest time for which the actual configuration of the membrane potential is ε close to a previous state,

$$t_{\rm tr} = \min\left\{t \middle| \max_i |v_i(t+T) - v_i(t)| < \varepsilon\right\},$$

where $1 \leqslant i \leqslant N$ and $1 \leqslant T \leqslant t-1$. The choice of the threshold is not crucial, since after the maximal distance is on the order of $1/N$, it starts converging exponentially fast to 0. Accordingly, by this procedure we determine not only the transient length but also the periodicity T of the asymptotic solution.

The dynamics (4) is usually simulated by starting from a random initial condition with the values of the membrane potentials $v_i(0)$ uniformly distributed in the interval $[-w,1]$. In the following we present a detailed analysis carried out for networks with $r_m=0.05$.

In order to deal with a more reliable quantity, we compute the average length of the transient $\langle t_{\rm tr}\rangle$ (here and in the following, angular brackets denote an average over both realizations of the network and different initial conditions of the membrane potentials). In Fig. 3, we have plotted the average transient vs G for two different values of the system size ($N=100$ and 200). For $G \lesssim 1$, $\langle t_{\rm tr}\rangle$ slightly decreases for increasing coupling strength. This is similar to what has been observed in the fully coupled network over the entire range of variation of G [4]. On the other hand, by further increasing the coupling strength $\langle t_{\rm tr}\rangle$ exhibits a sudden increase. More important is that the rate of increase is significantly larger when N doubles. Altogether these data suggest the existence of two distinct phases, approximately corresponding to G smaller and larger than 1.

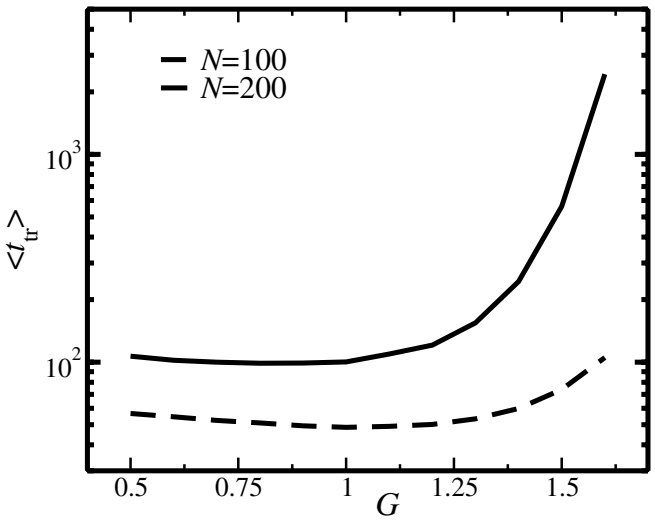

FIG. 3. Average transient length $\langle t_{\rm tr}\rangle$ vs G for two system sizes.

A more precise characterization of the dynamics is obtained by investigating the scaling behavior with N. In Fig. 4(a), we see that for $G=0.5$, the transient length increases linearly with the system size N, while the average period $\langle T\rangle$ of the asymptotic attractor remains almost constant. At the same time, in Fig. 4(b), we see that for $G=1.8$ and $G=2.5$, the transient grows exponentially fast. Finally, it turns out that for $G=2.5$ the average period also grows exponentially. We consider this a preliminary indication that at a larger coupling strength another transition may occur. However, here we focus our attention on the qualitative changes occurring for $G\approx 1$ where only the transient starts growing exponentially.

Another important point to be carefully investigated is the statistical properties of the transient dynamics. In particular, we start from the stationarity that can be analyzed by computing the so-called coefficient of variation (CV), which is determined by subdividing a time series $x(n)$, $n=1,2,\ldots,L$, into a sequence of windows of constant duration l, and then computing

$$\bar{x}(m) = \frac{1}{l}\sum_{i=(m-1)l+1}^{ml} x(i), \quad m = 1,2,\ldots,L/l,$$

$$\sigma(m) = \left[\frac{1}{l}\sum_{i=(m-1)l+1}^{ml} (x(i) - \bar{x}(m))^2\right]^{1/2}.$$

The coefficient of variation is thereby defined as

$$\mathrm{CV}(m) = \sigma(m)/\bar{x}(m). \tag{21}$$

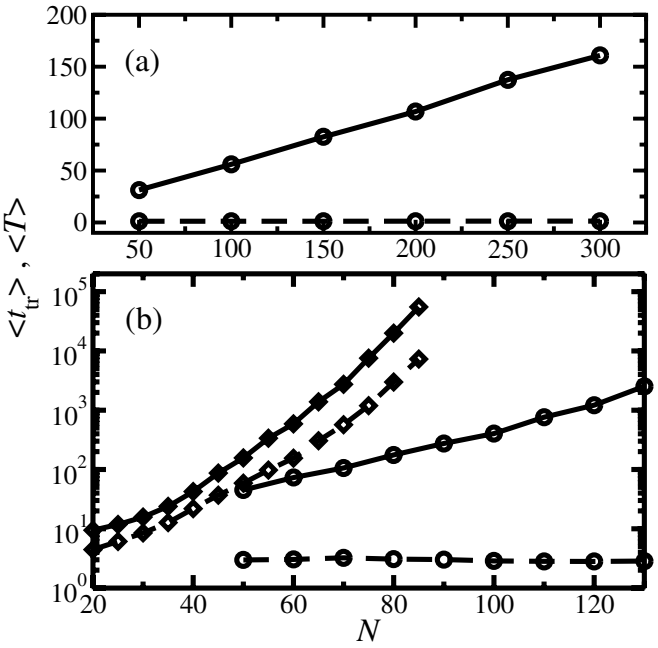

FIG. 4. Average length $\langle t_{tr} \rangle$ (solid line) of transient and corresponding period $\langle T \rangle$ of the periodic attractor (dashed line) vs system size: (a) $G=0.5$; (b) $G=1.8$ (circles), and $G=2.5$ (diamonds). Note in (b) the logarithmic scale of the vertical axis.

The parameter l must be chosen in such a way that each window contains a sufficient number of samples to reliably compute the local average and the standard deviation.

In our case, the time series of interest is the sequence of single neuron interspike intervals T, obtained by the iterating map (7). All intervals are recorded over a time window of length $l=10N$, so that each neuron fires on average ten times. In order to reduce statistical fluctuations, the CV has been further averaged over 100 different initial conditions for a fixed network realization. In Fig. 5, we have plotted the time evolution of $\langle \mathrm{CV}(n) \rangle_i$ for different values of G. Moreover, for each value of G, the behavior of $\langle \mathrm{CV}(n) \rangle_i$ is presented for two different network realizations to convince the reader that a further averaging on the disorder is not truly required to come to a conclusion about the stationarity of the regime. Indeed, the main point is that for $G<1$ the transient is nonstationary, as $\langle \mathrm{CV}(n) \rangle_i$ vanishes exponentially while approaching the periodic attractor. On the other hand, for $G \gtrsim 1.2$, $\langle \mathrm{CV}(n) \rangle_i$ approaches a finite value, thus confirming that the transient regime is stationary and one can thereby meaningfully speak of an invariant measure and pose the question of determining its correlation properties.

We have also performed other stationarity tests based, e.g., on the analysis of distributions of temporal distances of neighboring points in state space (e.g., see Ref. [14]). They confirm the stationarity of the transients above the transition and confirm the existence of a transition point in the interval $1.2<G<1.3$. Since these tools do not provide further insight, we do not comment further on their outcome.

The transient length strongly depends on the initial condition. In Fig. 6 we show the probability distribution function $P(t_{tr})$ for a given realization of the disorder in both phases.

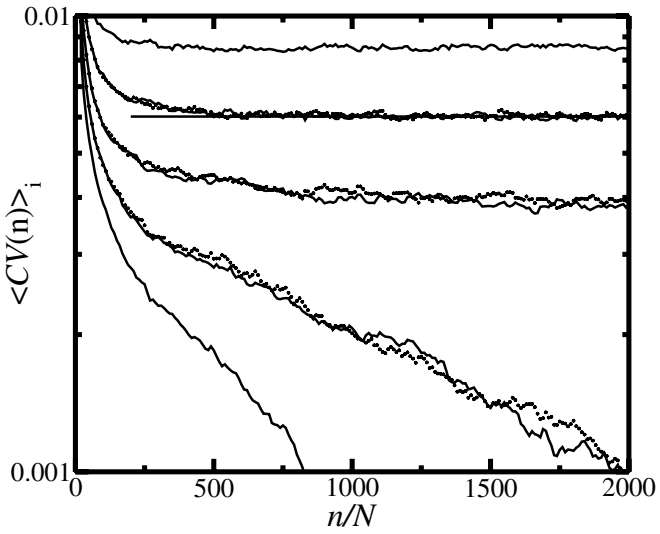

FIG. 5. Solid lines: The coefficient of variation as a function of integer time for $N=1000$ and (in ascending order starting from the bottom) $G=0.9, 1.0, 1.1, 1.2, 1.3$. Stars: The same for a different disorder realization and $G=1.0, 1.1, 1.2$. The straight line corresponds to the saturation value at $G=1.2$.

For small G, $P(t_{tr})$ can be confidently fitted with an inverse Gaussian (see the inset of Fig. 6), which is the typical statistical distribution of biased escape-time problems [15]. This confirms once more the nonstationarity of the corresponding transient dynamics, since it is driven by a systematic drift towards the asymptotic periodic state. Above the transition, $P(t_{tr})$ is Poissonian: the transient statistics can be therefore interpreted as a typical escape process through an activation barrier from a locally equilibrated system. Again, this evidence supports the conjectured stationarity of the transient dynamics for $G \gtrsim 1$ (in the large N limit).

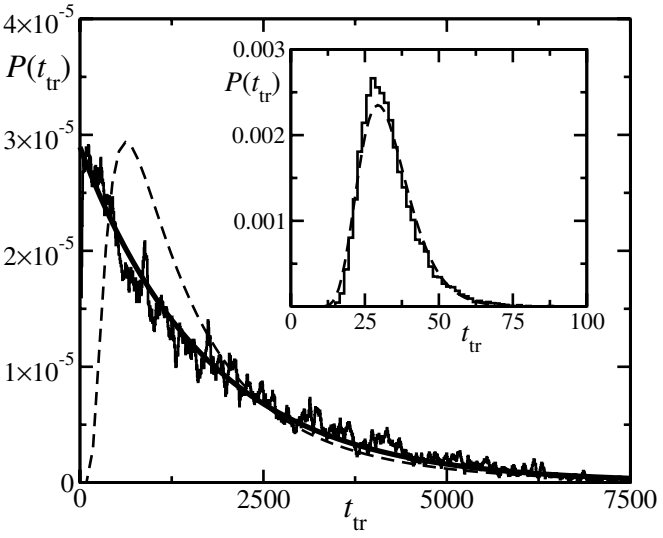

FIG. 6. Normalized histogram (random initial conditions at fixed disorder, $N=65$) of transient lengths for $G=2.1$. The solid curve is exponential; the dashed curve is an inverse Gaussian with equal mean and variance. The inset shows the distribution with an inverse Gaussian fit for $G=1$.

Finally, $P(t_{tr})$ does not change qualitatively for different realizations of disorder, although sizable quantitative differences can be found for small values of N. However, our simulations indicate that the probability distribution $P(t_{tr})$ is a self-averaging quantity since, upon increasing N, sample-to-sample fluctuations become increasingly small. This is absolutely clear for $G \approx < 1$, when it is possible to compute the transient time even for moderately large values of $N \sim \mathcal{O}(10^4)$. Above $G=1$, where direct simulations are almost undoable, there is, however, no reason to expect a qualitative change, given all the evidence of an ergodic dynamics.

Altogether, the transient dynamics observed for $G \approx > 1$: (i) is characterized by a negative Lyapunov exponent; (ii) is effectively stationary; (iii) lasts (with the system size) for exponentially long times. These are the distinguishing properties of "stable chaos," a phenomenon extensively investigated in coupled map lattices [8], where similar features of the transient statistics have been observed [16]. However, it is worth recalling that stable chaos has been observed also in chains of forced oscillators [17] and recently uncovered in the 1D hard-point gas of diatomic particles [18].

In all such instances, stable chaos is associated with the presence of discontinuities in phase space. In the coupled-map models, the discontinuities are transparent in the definition of the local piecewise linear maps [8]. In the hard-point gas they arise in connection with three-body collisions. Around any configuration leading to one such multiple collision, the ordering of the two-body collisions changes abruptly. The noncommutativity of the collision itself induces therefore a discontinuity in the dynamics that is conceptually similar to those postulated in the coupled-map lattices. The same happens in the present context. In fact, let us consider the time-evolved one-parameter family of configurations, $\mathbf{v}^{\nu}(t)=\{v_1^{\nu}(t), v_2^{\nu}(t), \ldots, v_k^{\nu}(t), v_{k+1}^{\nu}(t), \ldots, v_N^{\nu}(t)\}$ where $v_j^{\nu}(0)=u_j+\nu\delta_{jk}$ and δ_{jk} is the Kronecker delta function. It is easy to convince oneself that $\mathbf{v}_{\nu}(t)$ breaks into two disconnected parts when $v_k^{\nu}(t)=1$ if ν is such that $v_k^{\nu}(t)=v_{k+1}^{\nu}(t)$ and there is only one connection between neurons k and $k+1$. The discontinuity is due to the fact that only one of them inhibits the other. It is therefore interesting to verify that, in agreement with the past observations, the presence of discontinuities in the phase space is a condition for the onset of a stable chaos dynamics. If no anomalous transients arise for small coupling strengths, it is because the condition is necessary but not at all sufficient.

V. TWO DYNAMICAL PHASES

In this section we study the properties of the dynamical phases and perform a preliminary analysis of the transition. For $G \lesssim 1$, the evolution is similar to that of the fully coupled case. After a short transient time the system converges to a state characterized by a sequence of N spikes (emitted by the N neurons), which periodically repeats itself (see Fig. 7). All neurons fire with the same pace $[T(m)=\text{const.}]$, but their phases are no longer equispaced [i.e., $t_{ISI}(n)$ varies in time]. In other words, the asymptotic solution is a phase-locked, i.e. synchronized, state. In the following, this dynamical regime will be denoted *locked phase* (LP). The main difference with the fully coupled case is that different spike sequences are not equivalent to one another. In the limit of identically coupled neurons the dynamics is invariant under any permutation, but this is no longer true as soon as some degree of heterogeneity is introduced in the network connectivity. As a result, for $r_m \gtrsim 0$ there exists an exponentially large number of different periodic attractors. More precisely, the total number of attractors can be estimated to be of the order of $N!/(\Pi_{d=1}^{M} N_d!)$, where N_d is the number of neurons connected to the same (incoming and outgoing) neurons in the network and M is the number of these equivalence classes present in a given network realization.

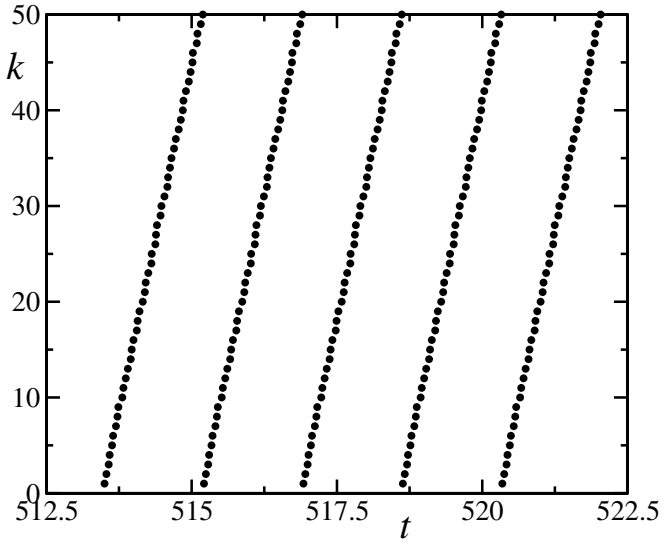

FIG. 7. Firing pattern (index of the firing neuron vs time) of a typical periodic attractor for $G=2$, $N=50$ in the LP; k is the index of the firing neuron.

For larger coupling strengths, an irregular dynamical regime arises that we call unlocked phase (UP), because the mutual ordering keeps changing during the entire transient, as one can, e.g., see in Fig. 8, where slow but systematic pattern adjustments can be seen in the whole time range.

One can better elucidate this dynamical phase by looking at the relative potential differences. Without prejudice of generality, we choose one of the N neurons, say neuron i, and consider the subsequence of its firing events. Given the spike emitted at time t, we compute the difference between the last ISI, $T^{(i)}$, of that neuron and the average ISI of the j neurons firing immediately before and after time t. We denote this time-dependent quantity by $\Delta\phi^{(i)}(t)$. The value of j has to be chosen neither too large, to avoid inclusion of spikes from the same neurons, nor too small, to get rid of local fluctuations. We have checked that the choice $j=5$ is a reasonable compromise. The integrated phaseshift $\Delta\Phi^{(i)}(t)=\int_0^t dt' \Delta\phi^{(i)} \times(t')$ is plotted in Fig. 9 for a generic initial condition and a typical realization of the disorder. In the LP, after a short transient, $\Delta\Phi^{(i)}$ collapses onto a constant value, which indicates that the system has converged to a periodic firing sequence with the neurons firing with the same pace. On the other hand, in the UP, $\Delta\Phi^{(i)}$ wanders erratically, performing a sort of unbiased random walk. We can indeed confirm that

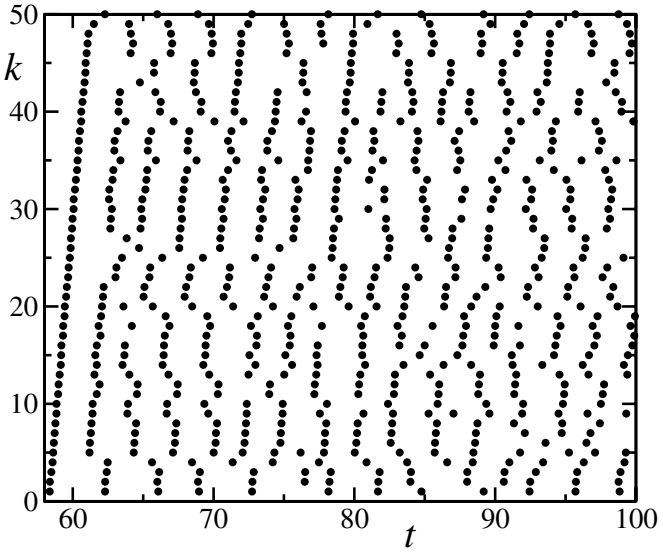

FIG. 8. Firing pattern for $G=2$, $N=50$ in the UP; k is the index of the firing neuron.

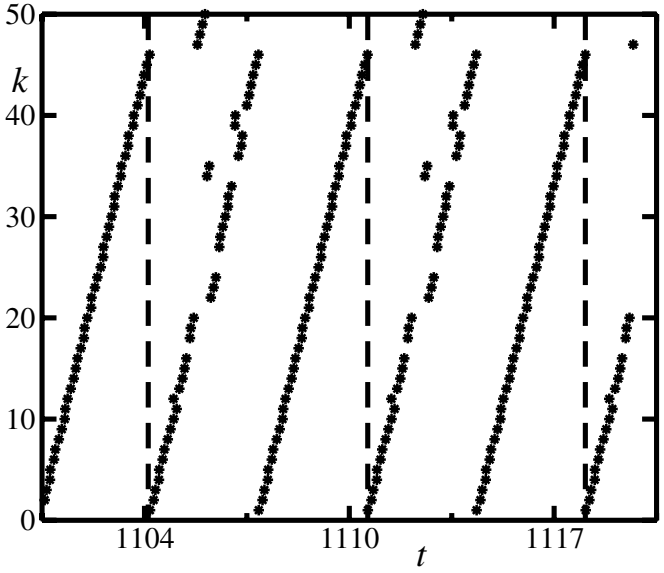

FIG. 10. Firing pattern associated with a periodic attractor in the UP for $G=2.0$, $N=50$. The period is indicated by the vertical lines.

at least for $G \lesssim 1.8$ and within statistical fluctuations all neurons are characterized by the same average firing rate.

A spontaneous symmetry breaking induced by disorder appears at larger coupling strengths when we can, e.g., find periodic orbits with different neurons exhibiting different firing rates (see Fig. 10). This phenomenon is, however, not connected with the onset of exponentially long transients that appears for significantly smaller G values.

Further information about the two dynamical phases can be gained from the introduction of a suitable space-time representation. Having verified that all neurons statistically behave in the same manner, we can split the entire spike series into sequences of N consecutive events and label the sequences with an index m, which naturally plays the role of time. On the other hand, the index i, labeling the position within a single sequence, plays the role of space. Finally, we introduce a binary variable $b(m,i)$ to distinguish two cases: whenever the neuron emitting the ith spike in the mth sequence is the same neuron which emits the ith spike in the $(m-1)$-st sequence, we set $b(m,i)=0$, otherwise $b(m,i)=1$. The resulting patterns are reported in Fig. 11, where 0, 1 are coded as black and white, respectively. In the UP, the pattern is very irregular and no order seems to emerge even after a very long time lapse. Conversely, in the LP, black tends to prevail quite soon, indicating that the system rapidly converges to a fixed firing sequence, i.e., to a periodic attractor. The most interesting features of this representation are the

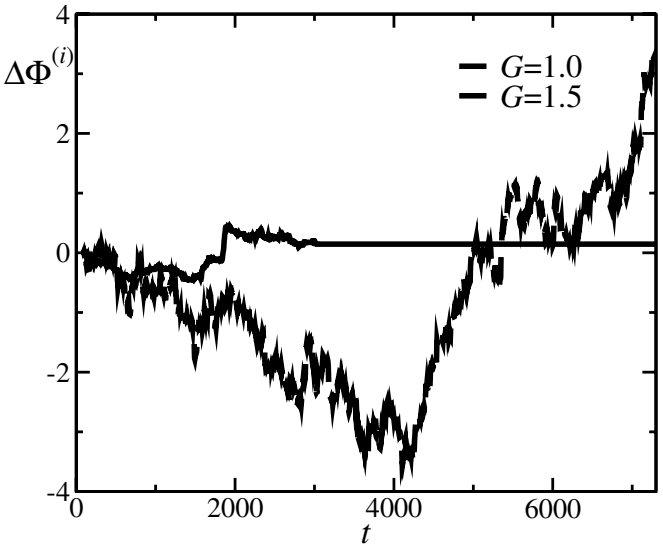

FIG. 9. Time evolution of the local phase difference $\Delta\Phi^{(i)}(t)$ for $G=1.0$ (solid line) and $G=1.5$ (dashed line). We consider a system with $N=1000$ and dilution $r_m=0.05$.

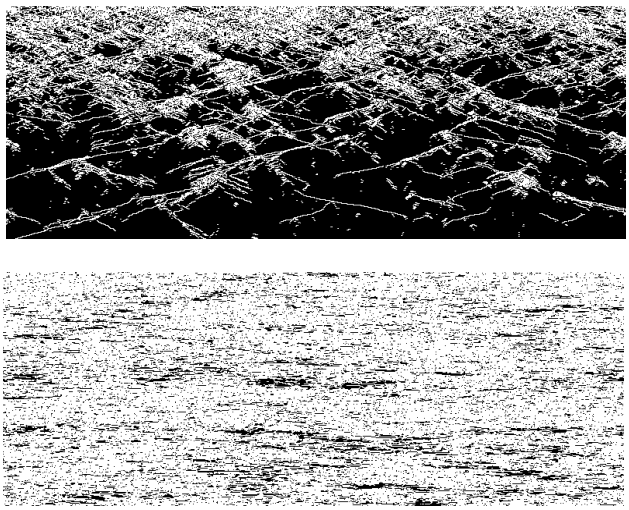

FIG. 11. Patterns associated with the two different phases of the dynamical system. The vertical axis (from top to down) reports the time, while the horizontal axis represents the index of successive firing neurons. The upper pattern refers to LP for $G=0.5$, and the lower to the transition region with $G=1.3$. In both cases a system with $N=801$ and dilution $r_m=0.05$ is considered.

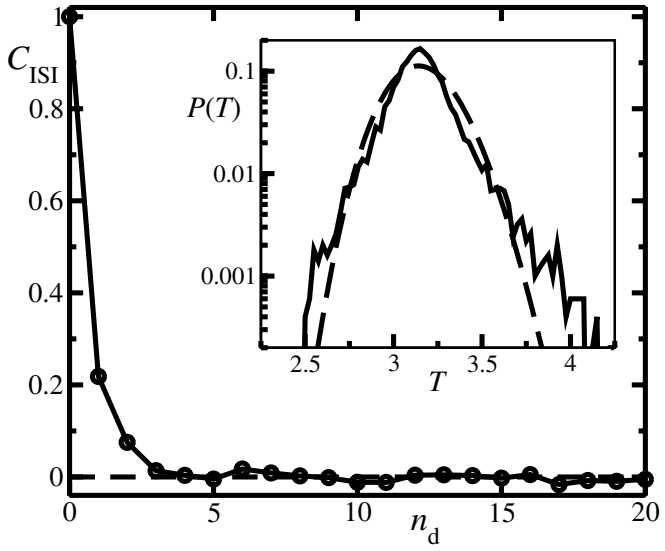

FIG. 12. The normalized autocorrelation C_{ISI} of the $T^{(i)}$ during transient for a single neuron i vs the integer delay for $N=1000$, $G=2.0$. The inset shows the corresponding distribution of the $T^{(i)}$ and an inverse Gaussian with the same mean and variance.

white *defects* propagating in the black background. They indicate that the firing rate of some neurons is temporarily slower or faster than that of the neighboring ones. These patterns are strongly reminiscent of a directed percolation (DP) transition. Actually, defects tend to be eliminated in the LP, which is analogous to the absorbing phase of DP. In turn, the UP shows similarities with the so-called "active" phase of DP, ruled by a persistent defect dynamics. It is remarkable that the dynamics of an almost globally coupled system exhibits distinctive features of one-dimensional systems with short-range interactions, as is the case of $1+1$ contact processes. The analogy appears less astonishing after recalling that the evolution of the fully coupled model is described by a suitable partial differential equation [see Eq. (18)]. However, including the role of disorder and proving a possible analogy with directed percolation is not an easy task. We prefer to leave the elucidation of this problem to future analyses and here we concentrate our efforts on obtaining a refined characterization of the two dynamical phases.

In particular, we have determined the distribution and the time autocorrelation function of the single-neuron interspike time interval $T^{(i)}(m)$. In the UP, the normalized autocorrelation function C_{ISI} is plotted in Fig. 12. It exhibits an exponentially fast decay, typical of both chaotic and stochastic regimes: memory is lost after typically 3 to 4 firing events. This quantitative confirmation of the irregularity is yet another element strengthening the analogy with stable chaos. The stochasticlike character of the evolution is also confirmed by the shape of the probability density function (PDF) $P(T^{(i)})$, which has a Poisson-type tail but also is not much different from an inverse Gaussian—a typical distribution encountered in neural dynamics [19].

Finally, given the evidence of the effective stochastic behavior, we develop a standard mean-field approach to characterize the behavior of the network in the large N limit. In particular, one can conveniently approximate the mean field with a deterministic drift plus a zero-average stochastic process. This amounts to replacing the initial model with the following stochastic equation (to be interpreted in the Ito sense, as the noise arises from a discrete-time equation),

$$\dot{v}_j = c - v_j - \frac{G(v_j+w)}{T} + \frac{G(v_j+w)}{(1-r_m)}\eta_j(t), \quad v \in [0,1), \tag{22}$$

where the time T is determined self-consistently, while $\eta_j(t)$ is a δ-correlated stochastic process

$$\langle \eta_i(0)\eta_j(t)\rangle = \frac{r_m(1-r_m)}{TN}\delta_{ij}\delta(t),$$

with δ_{ij} and $\delta(t)$ being the Kronecker and Dirac δ functions, respectively. In the thermodynamic limit the noise term vanishes and can therefore be neglected in the computation of average properties. In particular, by integrating the deterministic force field in Eq. (22)), one obtains an implicit equation for $T(G)$,

$$G = \frac{x}{1+x}\ln\frac{c-xw}{c-1-x(1+w)}, \tag{23}$$

where $x=G/T(G)$. This formula holds not only in the UP but also in the LP, because the main difference between the two regimes does not concern the noise amplitude, but its correlation properties. In fact, the relative diffusion of the generic neurons i and j depends on the fact that the stochastic signals η_i and η_j are not correlated with one another. If this is the case, the relative diffusion induced by the noise over a time equal to the average ISI is $1/\sqrt{N}$. Since, on the other hand, the average distance between consecutive neuron potentials is on the order of $1/N$, we conclude that for any finite G and large enough N the diffusion is sufficiently strong as to scramble the neurons. The smallness of the noise amplitude also explains why, at a coarse-grained level, the firing patterns appear almost periodic (see, e.g., Fig. 8). Now, in order to complete a self-consistency argument, it would be necessary to connect the changes in the neuron ordering with the correlation properties of the noise terms in Eq. (22)). Since different neurons have different connection trees, $\eta_i(t+T)$ will be decorrelated from $\eta_i(t)$ and, more important, $\eta_i(t+T)-\eta_j(t+T)$ will change with respect to the previous ISI. However, transforming these hand-waving arguments into a quantitative criterion for the identification of the critical value G_c, above which self-generated fluctuations can be robustly sustained, is not an easy task and we leave it to future studies. Here, we limit ourselves to stressing the relevant role played by correlations between neighboring neurons (i.e., those with the closest-to-threshold membrane potentials). Below G_c the neurons' rearrangement continues until a suitable ordering is reached, characterized by the property that neighboring neurons do not diffuse away from each other. The existence of exponentially long transients in the UP tells us that such an arrangement does not exist in the strong coupling regime.

The two-phase scenario here above described persists for a wide range of r_m values. While no qualitative changes are

expected to appear until r_m becomes so large that the network is decomposed into uncoupled blocks, we are unable to formulate any conjecture for the limit case $r_m \to 0$ due to the need of studying very large networks.

VI. CONCLUSIONS AND OPEN PROBLEMS

The main result of this paper is the observation that a network of leaky integrate-and-fire neurons can exhibit a pseudochaotic behavior in spite of an entirely negative Lyapunov spectrum. Previous studies [17] have identified in strong localized nonlinearities a necessary (and far from sufficient) condition for this phenomenon to exist. Discontinuities are indeed responsible for a sudden amplification of (finite-amplitude) perturbations and for the resulting irregular dynamics. In the models where this phenomenon was initially observed, the discontinuities are somehow artificial features of the local maps, but it has been recognized that they may also spontaneously emerge. This is the case of the hard-point diatomic gas, where discontinuities arise in the vicinity of three-body collisions [18]. Here, we have seen that they also occur in neuronal networks, in connection with changes in the spike ordering. However, when and why a discontinuity may be so important as to steadily sustain (in the thermodynamic limit) an irregular dynamics is still a completely open problem.

Another open question concerns the nature of the phase transition. Macroscopically, it manifests itself as a collective desynchronization, but there are difficulties in quantitatively describing the phenomenon. On one hand, it cannot be analyzed by looking at the linear stability of some solution, since linear stability is ensured above and below the transition. Moreover, the absence of local instabilities (standard deterministic chaos) makes questionable the concept of a transition point. In fact, the study of a partially analogous transition in a coupled map lattice revealed that regular and irregular phases are separated by a finite fuzzy region, rather than by a pointlike transition [20]. Perhaps the almost global coupling of the network studied in this paper may induce a standard transition scenario; the analogies with contact processes suggested by Fig. 9 indicate that this is a reasonable expectation. However for the moment, we must limit ourselves to observing that the scenario is robust against various modifications, such as the addition of further disorder accounting for the nonhomogeneous strength of the coupling and specific modifications of the network topology.

Recently, it has been pointed out that an irregular dynamics should significantly enhance information processing [21]. At variance with sparsely coupled chaotic networks, where chaos results from the balance of inhibition and excitation [22], we have found irregular firing patterns, characterized by a Poisson-type distribution of interspike intervals, in the presence of linear stability and the absence of excitation. It would be worth investigating if and how such a Lyapunov stable irregular dynamics is an effective tool for information processing. In the literature there is a growing evidence of recurrent motifs in the firing pattern (see, e.g., Ref. [23]), which suggests that phase locking may be a tool to encode information. In our model, recurrent motifs appear naturally in the UP and yet keep evolving, indicating a sort of information processing which certainly deserves a thorough investigation from this point of view.

ACKNOWLEDGMENTS

We thank T. Kreuz for performing the more elaborate stationarity tests. We further acknowledge MIUR for partial support within the PRIN05 project on "Dynamics and Thermodynamics of Systems with Long-range Interactions."

[1] S. H. Strogatz, Nature (London) **410**, 268 (2001).
[2] A. Destexhe, M. Rudolph, J.-M. Fellous, and T. J. Sejnowski, Neuroscience **107**, 13 (2001).
[3] N. Brunel and X.-J. Wang, J. Comput. Neurosci. **11**, 63 (2001).
[4] D. Z. Jin, Phys. Rev. Lett. **89**, 208102 (2002).
[5] Everywhere in this paper, we exclude the zero Lyapunov exponent corresponding to perturbations oriented along the trajectory itself. This will be automatically done, when in the following we implement a discrete-time mapping, by introducing a suitable Poincaré section.
[6] A. Zumdieck, M. Timme, T. Geisel, and F. Wolf, Phys. Rev. Lett. **93**, 244103 (2004).
[7] S. H. Strogatz and R. E. Mirollo, Phys. Rev. E **47**, 220 (1993).
[8] J. P. Crutchfield and K. Kaneko, Phys. Rev. Lett. **60**, 2715 (1988); A. Politi, R. Livi, G.-L. Oppo, and R. Kapral, Europhys. Lett. **22**, 571 (1993).
[9] F. Ginelli, R. Livi, A. Politi, and A. Torcini, Phys. Rev. E **67**, 046217 (2003).
[10] W. Gerstner and W. M. Kistler, *Spiking Neuron Models* (Cambridge University Press, Cambridge, 2002).
[11] N. Brunel and V. Hakim, Neural Comput. **11**, 1621 (1999).
[12] C. van Vreeswijk, Phys. Rev. E **54**, 5522 (1996).
[13] P. K. Mohanty and A. Politi, J. Phys. A **39**, L415 (2006).
[14] C. Rieke, K. Sternickel, R. G. Andrzejak, C. E. Elger, P. David, and K. Lehnertz, Phys. Rev. Lett. **88**, 244102 (2002).
[15] R. S. Chikara and J. L. Folks, *The Inverse Gaussian Distribution* (Marcel Dekker, New York, 1988).
[16] R. Livi, G. Martinez-Mekler, and S. Ruffo, Physica D **45**, 452 (1990).
[17] R. Bonaccini and A. Politi, Physica D **103**, 362 (1997).
[18] P. Cipriani, S. Denisov, and A. Politi, Phys. Rev. Lett. **94**, 244301 (2005); P. Cipriani and A. Politi, (unpublished).
[19] H. C. Tuckwell, *Introduction to Theoretical Neurobiology* (Cambridge University Press, New York, 1988).
[20] F. Cecconi, R. Livi, and A. Politi, Phys. Rev. E **57**, 3, 2703 (1998).
[21] N. Masuda and K. Aihara, Phys. Rev. Lett. **88**, 248101 (2002).
[22] C. van Vreeswijk and H. Sompolinsky, Science **274**, 5293, 1724 (1996).
[23] V. P. Zhigulin, Phys. Rev. Lett. **92**, 238701 (2004).